SUPPLEMENT

Estimating nitrogen and sulfur deposition across China during 2005-2020 based on multiple statistical models

Kaiyue Zhou[1], Wen Xu[3], Lin Zhang[4], Mingrui Ma[1], Xuejun Liu[3], Yu Zhao[1,2*]

1. State Key Laboratory of Pollution Control & Resource Reuse and School of the Environment, Nanjing University, Nanjing, Jiangsu 210023, China

2. Jiangsu Collaborative Innovation Center of Atmospheric Environment and Equipment Technology (CICAEET), Nanjing University of Information Science & Technology, Nanjing, Jiangsu 210044, China

3. Key Laboratory of Plant-Soil Interactions of MOE, College of Resources and Environmental Sciences, National Academy of Agriculture Green Development, China Agricultural University, Beijing 100193, China

4. Laboratory for Climate and Ocean-Atmosphere Sciences, Department of Atmospheric and Oceanic Sciences, School of Physics, Peking University, Beijing 100871, China

[*] Corresponding authors: Yu Zhao (yuzhao@nju.edu.cn)

Number of tables:6 Number of figures: 3

Table list

Table S1. Social-economical and geo-climatic conditions for six regions of China.

Table S2. Input variables in the RF algorithm.

Table S3. Comparison of the annual F_d of N and S in this and other studies (kg N/S ha^{-1} yr^{-1}).

Table S4. Comparisons of total deposition fluxes of different species between our study in China and two networks in other countries (kg N/S ha^{-1} yr^{-1}).

Table S5. The ratios of deposition of different forms and species for the six regions as well as eastern (SE+NC with Inner Mongolia excluded), western (NW+TP), and whole China.

Table S6. The annual emissions, deposition, and D/E by land use type, according to the latest Land-Use and Land-Cover Change (LUCC) information (http://www.resdc.cn/). "Urban" includes city/town and building categories, and "Rural" includes cropland and countryside categories.

Figure list

Figure S1. The RF algorithm monthly performance of CNEMC with the 10-fold cross validation. R^2 and RMSE are calculated with equations below the figure (the unit of RMSE are kg N/S ha^{-1} yr^{-1}).

Figure S2. The same as Figure S1 but for NNDMN.

Figure S3. China average total precipitation and 2m temperature data, from ECMWF: https://apps.ecmwf.int/datasets/data/interim-full-daily/levtype=sfc/.

TEXT SECTION: THE RF ALGORITHM AND EVALUATION

Basic algorithm of RF model

Decision tree (*tree*) is a basic classification and regression prediction model. It presents a tree structure that uses sample features as criteria and values as branches.

For *tree* = 1 to 1000:

- ✧ The samples and characteristic variables are randomly selected by the method of sampling with return (Liaw and Wiener, 2002);
- ✧ The best partition features and eigenvalues are found by minimizing the square error between the observation value and the mean value;
- ✧ The final output value of the base decision tree is obtained by the mean value of the response variables.

The model output is the average of the predictions of all trees.

The algorithm of RF regression model consists of a set of regression subtrees to form a set of combination models (Breiman, 2001), as expressed in Eq. (S1):

$$\bar{h}(x) = \frac{1}{N}\sum_{n=1}^{N}\{h(x_{\mathrm{k}}, \theta_{\mathrm{n}})\} \tag{S1}$$

where $h(x_{\mathrm{k}}, \theta_{\mathrm{n}})$ denotes the base decision tree of random forest; θ_n denotes a random vector with independent and identically distribution; x_k denotes an interpretation variable.

The best partition features j and eigenvalues s are determined by the square error minimization criterion, as expressed in Eq. (2) (Li et al., 2020):

$$\min_{j,s}[\min_{c_1}\sum_{xi\in R_1(j,s)}(y_i - c_1)^2 + \min_{c_2}\sum_{xi\in R_2(j,s)}(y_i - c_2)^2] \tag{S2}$$

The *min* of inner layer is the minimum value selected by each feature at its own feature level, i.e., the best partition feature point is selected for each feature; and the outer layer *min* is the selected feature with the smallest error at each feature level. R_1 and R_2 denote the two regions divided by partition condition (the

eigenvalue s of feature j is the logical judgment condition).

The model traverses all the characteristic variables j, scans the segmentation point s for the fixed partition variable, and selects the pair (j, s) that makes the Eq. (S2) reach the minimum value.

Determination of the relative importance of interpretation variables (RIV)

The idea of using RF to evaluate the RIV (dimensionless) is to see how much contribution of each feature has made to each tree, and finally we compare the contribution between features (Grömping, 2009; Wei et al., 2019). Conventional RIV calculation methods are divided into two types, i.e., calculated based on Gini index (RIV_j^{Gini}) and out-of-bag (OOB) data error rate (RIV_j^{OOB}).

(1) Calculation based on Gini index(RIV_j^{Gini}).

The calculation based on Gini index (GI) is expressed in Eq. (S3):

$$GI_m = \sum_{k=1}^{K} \hat{p}(1-\hat{p}) \tag{S3}$$

where K denotes the number of the features; $\hat{p}$ denotes the probability estimation value of node m sample belonging to class K.

The RIV to variable X_j on the node m, i.e., the Gini index change before and after node m branching, can be determined in Eq. (S4):

$$RIV_{jm}^{Gini} = GI_m - GI_l - GI_r \tag{S4}$$

where GI_l and GI_r denote the Gini index of two new nodes after m node splitting.

The final RIV is calculated with Eq. (S5):

$$RIV_j^{Gini} = \frac{1}{n}\sum_{i=1}^{n} RIV_{jm}^{Gini} \tag{S5}$$

(2) Calculation based on the OOB error rate (RIV_j^{OOB}).

✧ In each tree of RF, the training self-service samples are randomly selected to build the tree, and the prediction error rate of the out of bag data (OOB) is calculated.

- ✧ The observation value of the variable X_j is randomly replaced, and the prediction error rate of OOB is calculated again.
- ✧ Finally, the difference between the two OOB error rates is calculated.

After standardization, the mean value in all trees is the RIV_j^{OOB} of variable X_j.

Table S1. Social-economical and geo-climatic conditions for six regions of China.

Regions	The percentage of China		Climatic conditions
	Area	GDP	
NC	10%	28%	temperate monsoon climate
NE	6%	9%	temperate monsoon climate
NW	35%	5%	temperate continental climate
SE	13%	46%	subtropical monsoon climate
SW	14%	12%	subtropical and plateau monsoon climates
TP	20%	0.5%	alpine mountain climate

Table S2. Input variables in the RF algorithm.

Class	Symbol	Description
Response variable	F_d	Observed ground-level concentration×modeled V_d, kg N/S ha^{-1} yr^{-1}
Interpretation variables		
Satellite-derived VCD	SAT	Satellite-derived vertical columns densities, 10^{15}mol cm^{-2}
Meteorology	sp	Surface pressure
	wind	Wind direction, °
	t2m	Temperature at 2 meters, K
	pre	Precipitation, mm
	si10	Wind speed at 10 meters, m s^{-1}
	blh	Boundary layer height, m
	tcw	Total column water, kg m^{-2}
	tclw	Total column liquid water, kg m^{-2}
	d2m	Dewpoint temperature at 2 meters, K
	tco3	Total column ozone, kg m^{-2}
	kx	K index, K
	zust	Friction velocity, m s^{-1}
	gwd	Gravity wave dissipation, J m^{-2}
	tcc	Total cloud cover
	bld	Boundary layer dissipation, J m^{-2}
	magss	Magnitude of turbulent surface stress, N m^{-2} s
Emissions	eNOX	Emission of NO_X, Mg $grid^{-1}$
	eNH3	Emission of NH_3, Mg $grid^{-1}$
	eSO2	Emission of SO_2, Mg $grid^{-1}$
Geography	Lai_lv	Leaf area index, low vegetation, m^2 m^{-2}
	lai_hv	Leaf area index, high vegetation, m^2 m^{-2}
	ROAD	Road density, km $grid^{-1}$
	DEM	Elevation, m
	LUCC	Land use type proportion, %
	GDP	Gross Domestic Product, 10000 yuan km^{-2}
	POP	Population density, people km^{-2}
Modeled concentrations from CTM	c_species	Including HNO_3, NH_3, NH_4^+, NO_3^-, SO_4^{2-}, ug m^{-3}

Table S3. Comparison of the annual F_d of N and S in this and other studies (kg N/S ha^{-1} yr^{-1}).

Reference	Study region	Study period	Dry deposition							Wet/bulk deposition			Total deposition	
			NO_2	HNO_3	NO_3^-	NH_3	NH_4^+	SO_2	SO_4^{2-}	NH_4^+	NO_3^-	SO_4^{2-}	N	S
This study	China	2005-2020	3.4	5.3	1.7	10.3	4.2	15.5	1.2	3.3	4.6	6.4	32.9	23.1
Nowlan et al. (2014)	China	2005-2007	0.2											
Lye and Tian (2007)	China	2003	2.9							7.1	2.8		12.9	
Jia et al. (2014)	China	1980-2010												
Jia et al. (2016)	China	2005-2014	0.6	1.1	0.1	5.4	0.3			13.9				
Tan et al. (2022)	China	2010								4.2	3.4			
Itahashi et al. (2018)	China	2010								3.5	2.5			
Zhao et al. (2017)	China	2008-2012	0.3	1.7	1.0	0.5	2.6			6.6	3.4		18.1	
Xu et al. (2015)	China	2010-2014	0.2-9.8	0.2-16.6	0.1-4.5	0.5-16.0	0.1-11.7			1.0-19.1	0.5-20.1		39.9	
Xu et al. (2019)	China	2010-2015	3.1	5.2	1.4	9.6	3.7			11.4	10.3			
Wen et al. (2020)	China	2011-2018			22.5					19.4				
Pan et al. (2012)	Northern China	2007-2010	0.8-4.5		2.2-3.1	8.1-64.2	1.7-5.5			10.3-22.0	3.4-10.2		60.6	
Pan et al. (2013)	Northern China	2007-2010						32.4	12.8			19.6		64.8
Zhu et al. (2015)	China	2013								7.3	5.9			
Yu et al. (2016)	China	2009-2014									32.9	116.0		
Yu et al. (2019)	China	1985-2015	0.8	2.0	2.7	0.5	4.3			5.9	4.2		20.4	
Li et al. (2019)	China	2010										71.5		
Li et al. (2020)	China	2011-2016								5.9	13.3	33.4		
Liu et al. (2016a)	Southwest China	2003-2013								17.5	8.2	21.7		
Liu et al. (2016b)	China	2003-2014								6.8	5.4			
Liu et al. (2016c)	China	2000-2013										23.0		
Liu et al. (2017a)	China	2010-2012									5.8			

Table S3 (continued)

Reference	Study region	Study period	Dry deposition							Wet/bulk deposition			Total deposition	
			NO_2	HNO_3	NO_3^-	NH_3	NH_4^+	SO_2	SO_4^{2-}	NH_4^+	NO_3^-	SO_4^{2-}	N	S
Liu et al. (2017b)	China	2012			1.5									
Liu et al. (2021)	China	2008-2016								6.5				
Luo et al. (2016)	China	2010-2012						2.3-26.5	0.5-3.4					
Ge et al. (2014)	China	2007								9.1	9.1	48.8	35.0	83.3
Kuribayashi et al. (2012)	China	2001-2005						23.5	3.8			49.4		
Zhang et al. (2016)												10.4		
Zhang et al. (2017)	China	2007-2014	0.005-8.54											
Zhou et al. (2021)	China	2013-2018	2.1-3.1					7.5-18.4						
Qiao et al. (2015b)	Sichuan Province, China										0.3	2.8		
Qiao et al. (2015a)	Sichuan Province, China	2010-2011								1.4	1.3	8.1		
Zhang et al. (2022)	Tibetan Plateau									2.6	7.4			
Larssen et al. (2011)	Four Chinese Study Sites	2001-2004								0.4-0.9	0.2-0.5	0.9-1.9	0.4-2.5	1.5-10.5
Jiang et al. (2020)	Hunan Province, China	2015-2016						8.6				18.2		26.8

Table S4. Comparisons of total deposition fluxes of different species between our study in China and two networks in other countries (kg N/S ha^{-1} yr^{-1}).

	Period	RDN	OXN	N	S
USA	1990-2020	2.0	3.0	5.0	5.4
Europe	2000-2019	1.1	1.1	2.2	1.4
China	2005-2020	20.2	15.2	35.4	25.9

Table S5. The ratios of deposition of different forms and species for the six regions as well as eastern (SE+NC with Inner Mongolia excluded), western (NW+TP), and whole China.

Regions		NC	NE	NW	SE	SW	TP	Eastern China	Western China	Whole China
Nitrogen	$R_{dry/wet}$	1.9	2.9	2.5	1.4	2.0	2.6	1.6	2.5	2.3
	$R_{RDN/OXN}$	1.3	1.2	1.4	1.2	1.1	1.7	1.2	1.5	1.3
Sulfur	$R_{dry/wet}$	1.2	1.9	2.4	0.8	1.1	3.7	0.9	2.7	1.8

Table S6. The annual emissions, deposition, and D/E by land use type, according to the latest Land-Use and Land-Cover Change (LUCC) information(http://www.resdc.cn/). "Urban" includes city/town and building categories, and "Rural" includes cropland and countryside categories.

LUCC		Cropland	Forest	Grassland	Water body	City/town	Countryside	Building	Unused land	**Urban**	**Rural**
Emissions (kg N/S ha^{-1} yr^{-1})	NO_X	27.3	8.9	4.5	22.7	86.1	53.8	62.0	1.4	78.7	29.1
	NH_3	22.3	8.8	3.1	11.4	29.3	34.1	20.6	1.1	26.6	23.1
	SO_2	28.2	9.9	5.2	25.0	68.0	44.7	70.9	1.3	68.9	29.3
Deposition (kg N/S ha^{-1} yr^{-1})	Dry OXN	13.1	13.0	8.9	9.9	15.5	14.3	14.2	7.2	15.1	13.2
	Wet OXN	7.4	5.0	3.9	5.7	9.0	8.5	7.5	2.9	8.6	7.5
	Total OXN	20.5	18.0	12.8	15.7	24.5	22.8	21.7	10.2	23.6	20.7
	Dry RDN	16.8	13.8	13.7	14.6	19.1	19.3	17.0	13.8	18.4	17.0
	Wet RDN	8.7	5.8	4.8	7.3	11.2	11.9	10.2	4.6	10.9	8.9
	Total RDN	25.5	19.6	18.5	22.0	30.3	31.2	27.2	18.3	29.3	25.9
	Dry N	29.9	26.8	22.6	24.6	34.5	33.6	31.2	21.0	33.5	30.2
	Wet N	16.1	10.8	8.7	13.0	20.2	20.4	17.7	7.5	19.5	16.4
	Total N	46.0	37.6	31.3	37.6	54.8	54.0	48.9	28.5	53.0	46.6
	Dry S	17.8	17.3	16.0	17.6	17.4	18.0	18.6	16.0	17.8	17.8
	Wet S	14.9	12.9	5.7	10.2	18.1	17.8	16.6	4.0	17.6	15.1
	Total S	32.7	30.2	21.7	27.8	35.5	35.8	35.1	20.1	35.4	32.9
D/E	Dry OXN	0.48	1.46	1.99	0.44	0.18	0.27	0.23	5.26	0.19	0.45
	Wet OXN	0.27	0.56	0.88	0.25	0.10	0.16	0.12	2.14	0.11	0.26
	Total OXN	0.75	2.03	2.87	0.69	0.28	0.42	0.35	7.40	0.30	0.71
	Dry RDN	0.75	1.58	4.34	1.29	0.65	0.57	0.83	12.23	0.69	0.74
	Wet RDN	0.39	0.66	1.52	0.64	0.38	0.35	0.50	4.05	0.41	0.39
	Total RDN	1.15	2.24	5.86	1.93	1.03	0.91	1.32	16.28	1.10	1.12
	Dry S	0.63	1.75	3.10	0.70	0.26	0.40	0.26	12.46	0.26	0.61
	Wet S	0.53	1.30	1.10	0.41	0.27	0.40	0.23	3.14	0.26	0.52
	Total S	1.16	3.05	4.21	1.11	0.52	0.80	0.50	15.61	0.51	1.12

Figure S1. The RF algorithm monthly performance of CNEMC with the 10-fold cross validation. R^2 and RMSE are calculated with equations below the figure (the unit of RMSE are kg N/S ha^{-1} yr^{-1}).

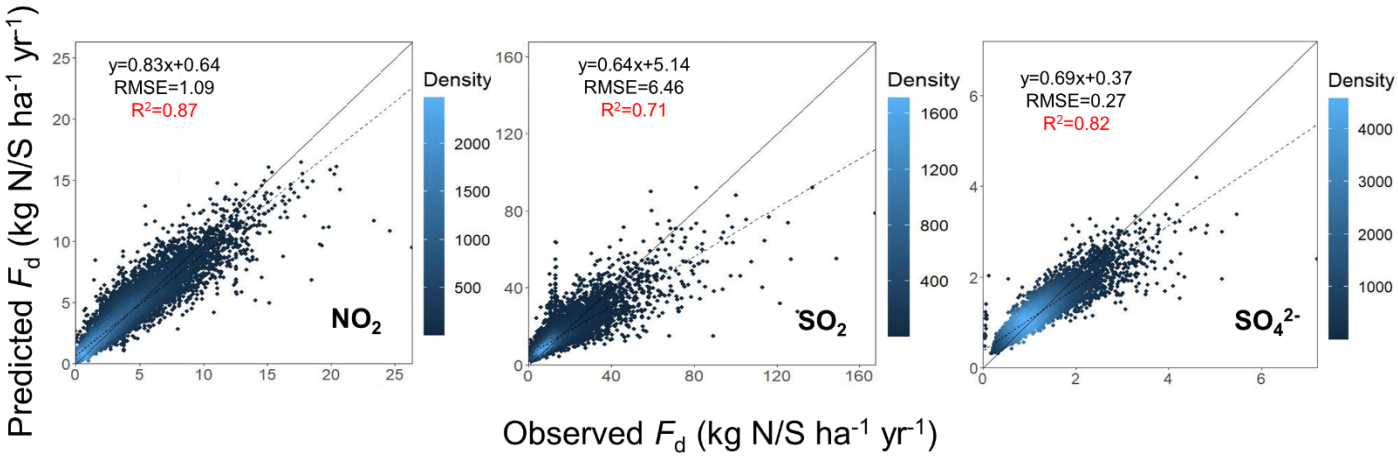

Note: The R^2, RMSE, MPE and RPE were calculated using following equations (*P* and *O* indicates the results from prediction and observation, respectively):

$$R^2 = \frac{\sum_{i=1}^{n}(P_i - \overline{O})^2}{\sum_{i=1}^{n}(O_i - \overline{O})^2} \qquad \text{RMSE} = \sqrt{\frac{1}{n}\sum_{i=1}^{n}(P_i - O_i)^2}$$

Figure S2. The same as Figure S1 but for NNDMN.

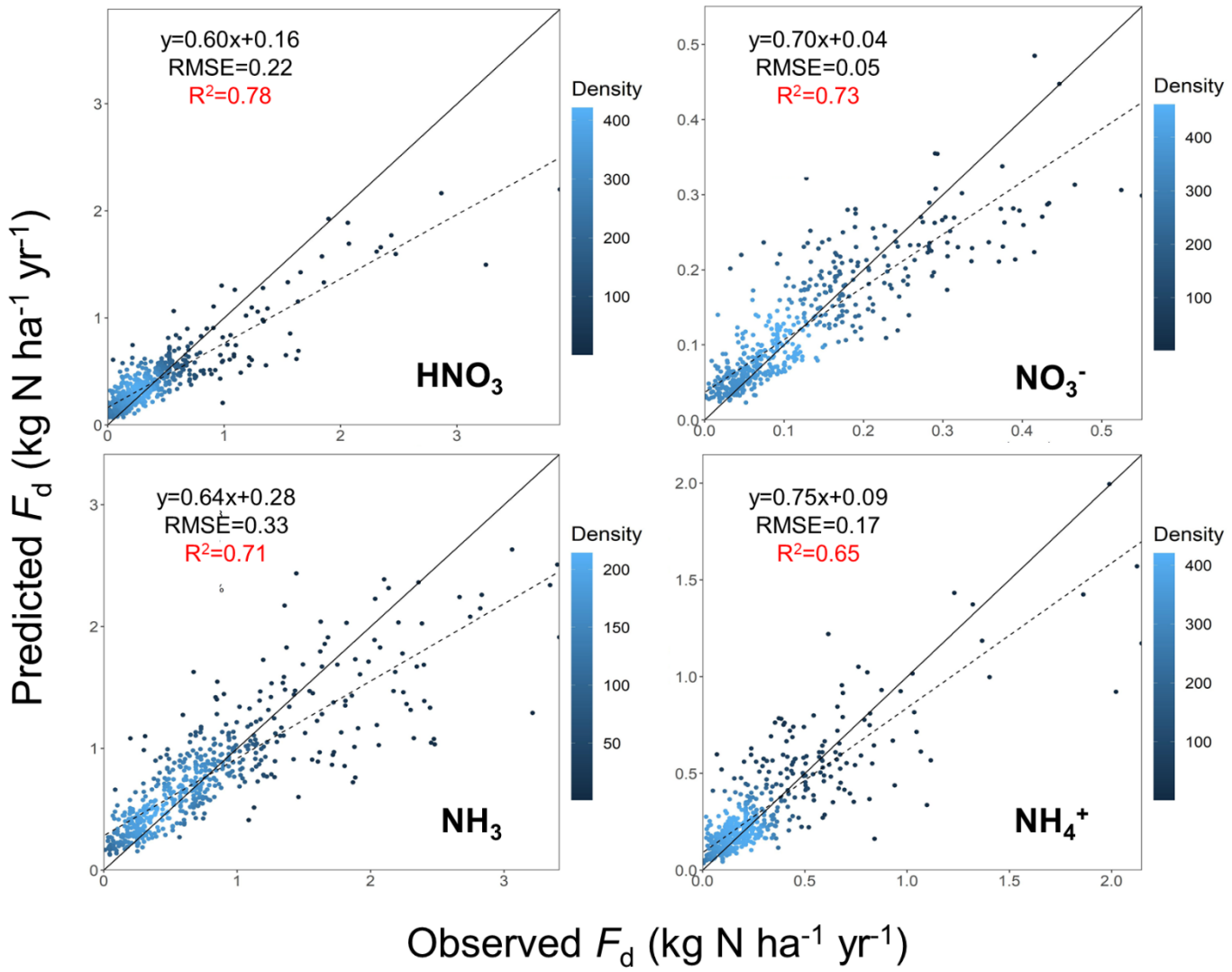

Figure S3. China average total precipitation and 2m temperature data, from ECMWF: https://apps.ecmwf.int/datasets/data/interim-full-daily/levtype=sfc/.

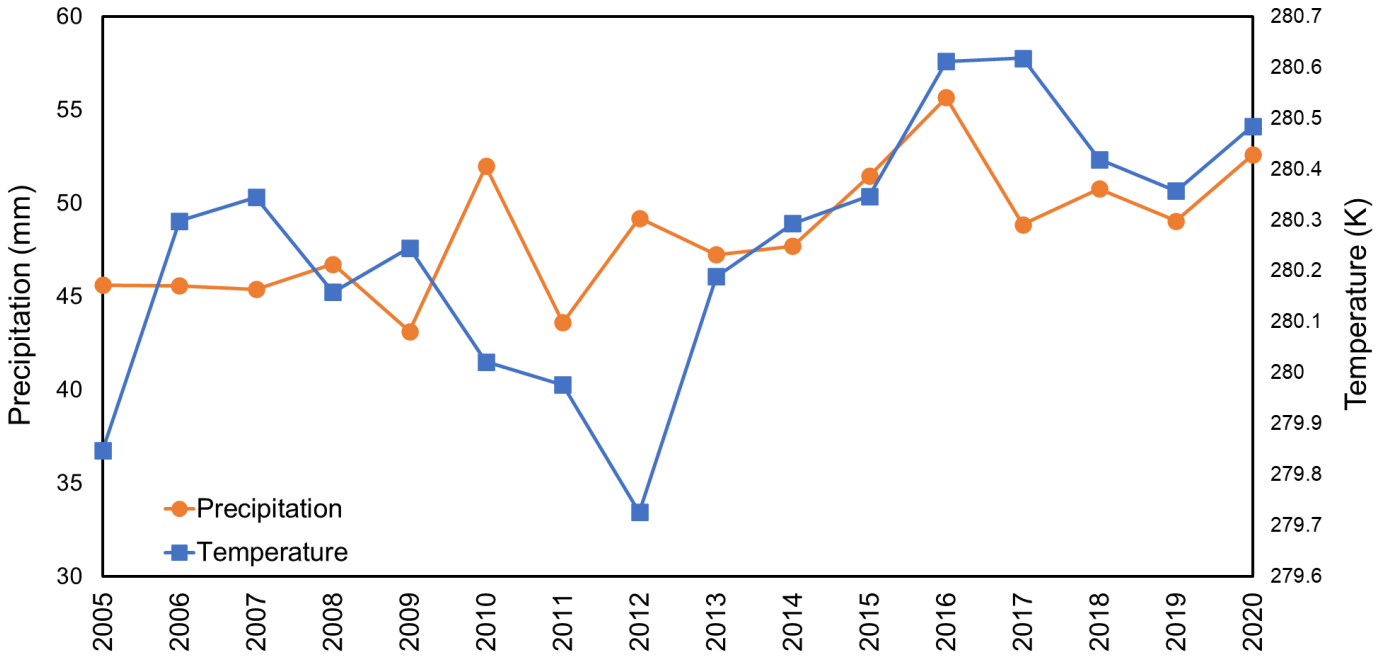

References

Breiman, L.: Random forests, Mach. Learn., 45, 5-32, https://doi.org/10.1023/a:1010933404324, 2001.

Ge, B. Z., Wang, Z. F., Xu, X. B., Wu, J. B., Yu, X. L., and Li, J.: Wet deposition of acidifying substances in different regions of China and the rest of East Asia: modeling with updated NAQPMS, Environ. Pollut., 187, 10-21, https://doi.org/10.1016/j.envpol.2013.12.014, 2014.

Itahashi, S., Yumimoto, K., Uno, I., Hayami, H., Fujita, S.-i., Pan, Y., and Wang, Y.: A 15-year record (2001–2015) of the ratio of nitrate to non-sea-salt sulfate in precipitation over East Asia, Atmos. Chem. Phys., 18, 2835-2852, https://doi.org/10.5194/acp-18-2835-2018, 2018.

Jia, Y., Yu, G., Gao, Y., He, N., Wang, Q., Jiao, C., and Zuo, Y.: Global inorganic nitrogen dry deposition inferred from ground- and space-based measurements, Sci. Rep., 6, 19810, https://doi.org/10.1038/srep19810, 2016.

Jia, Y., Yu, G., He, N., Zhan, X., Fang, H., Sheng, W., Zuo, Y., Zhang, D., and Wang, Q.: Spatial and decadal variations in inorganic nitrogen wet deposition in China induced by human activity, Sci. Rep., 4, 3763, https://doi.org/10.1038/srep03763, 2014.

Jiang, W., Zhu, X., Shen, J., Huang, Z., Gong, D., Li, Y., and Wu, J.: Atmospheric sulfur deposition in a paddy rice region in the hilly region in central china, China Environ. Sci., 40, 4848-4856, http://www.zghjkx.com.cn/EN/Y2020/V40/I11/4848, 2020.

Kuribayashi, M., Ohara, T., Morino, Y., Uno, I., Kurokawa, J.-i., and Hara, H.: Long-term trends of sulfur deposition in East Asia during 1981–2005, Atmos. Environ., 59, 461-475, https://doi.org/10.1016/j.atmosenv.2012.04.060, 2012.

Larssen, T., Duan, L., and Mulder, J.: Deposition and leaching of sulfur, nitrogen and calcium in four forested catchments in China: implications for acidification, Environ. Sci. Technol., 45, 1192-1198, https://doi.org/10.1021/es103426p, 2011.

Li, R., Cui, L., Fu, H., Zhao, Y., Zhou, W., and Chen, J.: Satellite-Based Estimates of Wet Ammonium (NH_4-N) Deposition Fluxes Across China during 2011-2016 Using a Space-Time Ensemble Model, Environ. Sci. Technol., 54, 13419-13428, https://doi.org/10.1021/acs.est.0c03547, 2020.

Li, R., Cui, L., Zhao, Y., Meng, Y., Kong, W., and Fu, H.: Estimating monthly wet sulfur (S) deposition flux over China using an ensemble model of improved machine learning and geostatistical approach, Atmos. Environ., 214, 116884, https://doi.org/10.1016/j.atmosenv.2019.116884, 2019.

Liaw, A. and Wiener, M.: Classification and Regression by randomForest, 18-22,

Liu, L., Zhang, X., and Lu, X.: The composition, seasonal variation, and potential sources of the atmospheric wet sulfur (S) and nitrogen (N) deposition in the southwest of China, Environ Sci. Pollut. Res. Int., 23, 6363-6375, https://doi.org/10.1007/s11356-015-5844-1, 2016a.

Liu, L., Zhang, X., Wang, S., Lu, X., and Ouyang, X.: A review of spatial variation of inorganic nitrogen (N) wet deposition in China, PLoS One, 11, e0146051, https://doi.org/10.1371/journal.pone.0146051, 2016b.

Liu, L., Zhang, X., Wang, S., Zhang, W., and Lu, X.: Bulk sulfur (S) deposition in China, Atmos. Environ., 135, 41-49, https://doi.org/10.1016/j.atmosenv.2016.04.003, 2016c.

Liu, L., Yang, Y., Xi, R., Zhang, X., Xu, W., Liu, X., Li, Y., Liu, P., and Wang, Z.: Global wet-reduced nitrogen deposition derived from combining satellite measurements with output from a chemistry transport model, J. Geophys. Res., 126, https://doi.org/10.1029/2020jd033977, 2021.

Liu, L., Zhang, X., Xu, W., Liu, X., Lu, X., Chen, D., Zhang, X., Wang, S., and Zhang, W.: Estimation of monthly bulk nitrate deposition in China based on satellite NO_2 measurement by the Ozone Monitoring Instrument, Remote Sens. Environ., 199, 93-106, https://doi.org/10.1016/j.rse.2017.07.005, 2017a.

Liu, L., Zhang, X., Zhang, Y., Xu, W., Liu, X., Zhang, X., Feng, J., Chen, X., Zhang, Y., Lu, X., Wang, S., Zhang, W., and Zhao, L.: Dry particulate nitrate deposition in China, Environ. Sci. Technol., 51, 5572-5581, https://doi.org/10.1021/acs.est.7b00898, 2017b.

Luo, X., Pan, Y., Goulding, K., Zhang, L., Liu, X., and Zhang, F.: Spatial and seasonal variations of atmospheric sulfur concentrations and dry deposition at 16 rural and suburban sites in China, Atmos. Environ., 146, 79-89, https://doi.org/10.1016/j.atmosenv.2016.07.038, 2016.

Lye, C. and Tian, H.: Spatial and temporal patterns of nitrogen deposition in China: Synthesis of observational data, J. Geophys. Res., 112, https://doi.org/10.1029/2006jd007990, 2007.

Nowlan, C. R., Martin, R. V., Philip, S., Lamsal, L. N., Krotkov, N. A., Marais, E. A., Wang, S., and Zhang, Q.: Global dry deposition of nitrogen dioxide and sulfur dioxide inferred from space-based measurements, Global Biogeochem. Cycles, 28, 1025-1043, https://doi.org/10.1002/2014gb004805, 2014.

Pan, Y. P., Wang, Y. S., Tang, G. Q., and Wu, D.: Wet and dry deposition of atmospheric nitrogen at ten sites in Northern China, Atmos. Chem. Phys., 12, 6515-6535, https://doi.org/10.5194/acp-12-6515-2012, 2012.

Pan, Y. P., Wang, Y. S., Tang, G. Q., and Wu, D.: Spatial distribution and temporal variations of atmospheric sulfur deposition in Northern China: insights into the potential acidification risks, Atmos. Chem. Phys., 13, 1675-1688, https://doi.org/10.5194/acp-13-1675-2013, 2013.

Qiao, X., Xiao, W., Jaffe, D., Kota, S. H., Ying, Q., and Tang, Y.: Atmospheric wet deposition of sulfur and nitrogen in Jiuzhaigou National Nature Reserve, Sichuan Province, China, Sci. Total Environ., 511, 28-36, https://doi.org/10.1016/j.scitotenv.2014.12.028, 2015a.

Qiao, X., Tang, Y., Hu, J., Zhang, S., Li, J., Kota, S. H., Wu, L., Gao, H., Zhang, H., and Ying, Q.: Modeling dry and wet deposition of sulfate, nitrate, and ammonium ions in Jiuzhaigou National Nature Reserve, China using a source-oriented CMAQ model: Part I. Base case model results, Sci. Total Environ., 532, 831-839, https://doi.org/10.1016/j.scitotenv.2015.05.108, 2015b.

Tan, J., Su, H., Itahashi, S., Tao, W., Wang, S., Li, R., Fu, H., Huang, K., Fu, J. S., and Cheng, Y.: Quantifying the wet deposition of reactive nitrogen over China: Synthesis of observations and models, Sci. Total Environ., 851, 158007, https://doi.org/10.1016/j.scitotenv.2022.158007, 2022.

Wen, Z., Xu, W., Li, Q., Han, M., Tang, A., Zhang, Y., Luo, X., Shen, J., Wang, W., Li, K., Pan, Y., Zhang, L., Li, W., Collett, J. L., Jr., Zhong, B., Wang, X., Goulding, K., Zhang, F., and Liu, X.: Changes of nitrogen deposition in China from 1980 to 2018, Environ. Int., 144, 106022, https://doi.org/10.1016/j.envint.2020.106022, 2020.

Xu, W., Zhang, L., and Liu, X.: A database of atmospheric nitrogen concentration and deposition from the nationwide monitoring network in China, Sci. Data, 6, 51, https://doi.org/10.1038/s41597-019-0061-2, 2019.

Xu, W., Luo, X. S., Pan, Y. P., Zhang, L., Tang, A. H., Shen, J. L., Zhang, Y., Li, K. H., Wu, Q. H., Yang, D. W., Zhang, Y. Y., Xue, J., Li, W. Q., Li, Q. Q., Tang, L., Lu, S. H., Liang, T., Tong, Y. A., Liu, P., Zhang, Q., Xiong, Z. Q., Shi, X. J., Wu, L. H., Shi, W. Q., Tian, K., Zhong, X. H., Shi, K., Tang, Q. Y., Zhang, L. J., Huang, J. L., He, C. E., Kuang, F. H., Zhu, B., Liu, H., Jin, X., Xin, Y. J., Shi, X. K., Du, E. Z., Dore, A. J., Tang, S., Collett, J. L., Goulding, K., Sun, Y. X., Ren, J., Zhang, F. S., and Liu, X. J.: Quantifying atmospheric nitrogen deposition through a nationwide monitoring network across China, Atmos. Chem. Phys., 15, 12345-12360, https://doi.org/10.5194/acp-15-12345-2015, 2015.

Yu, G., Jia, Y., He, N., Zhu, J., Chen, Z., Wang, Q., Piao, S., Liu, X., He, H., Guo, X., Wen, Z., Li, P., Ding, G., and Goulding, K.: Stabilization of atmospheric nitrogen deposition in China over the past decade, Nature Geosci., 12, 424-431, https://doi.org/10.1038/s41561-019-0352-4, 2019.

Yu, H., He, N., Wang, Q., Zhu, J., Xu, L., Zhu, Z., and Yu, G.: Wet acid deposition in Chinese natural and agricultural ecosystems: Evidence from national-scale monitoring, J. Geophys. Res.: Atmospheres, 121, 10,995-911,005, https://doi.org/10.1002/2015jd024441, 2016.

Zhang, B., Li, Z., Feng, Q., Gui, J., Zhao, Y., and Zhang, B.: Environmental significance of atmospheric nitrogen deposition in the transition zone between the Tibetan Plateau and arid region, Chemosphere, 307, 136096, https://doi.org/10.1016/j.chemosphere.2022.136096, 2022.

Zhang, L., Shao, J., Lu, X., Zhao, Y., Hu, Y., Henze, D. K., Liao, H., Gong, S., and Zhang, Q.: Sources and processes affecting fine particulate matter pollution over North China: An adjoint analysis of the Beijing APEC period, Environ. Sci. Technol., 50, 8731-8740, https://doi.org/10.1021/acs.est.6b03010, 2016.

Zhang, X. Y., Lu, X. H., Liu, L., Chen, D. M., Zhang, X. M., Liu, X. J., and Zhang, Y.: Dry deposition of NO_2 over China inferred from OMI columnar NO_2 and atmospheric chemistry transport model, Atmos. Environ., 169, 238-249, https://doi.org/10.1016/j.atmosenv.2017.09.017, 2017.

Zhao, Y., Zhang, L., Chen, Y., Liu, X., Xu, W., Pan, Y., and Duan, L.: Atmospheric nitrogen deposition to China: A model analysis on nitrogen budget and critical load exceedance, Atmos. Environ., 153, 32-40, https://doi.org/10.1016/j.atmosenv.2017.01.018, 2017.

Zhou, K., Zhao, Y., Zhang, L., and Xi, M.: Declining dry deposition of NO_2 and SO_2 with diverse spatiotemporal patterns in China from 2013 to 2018, Atmos. Environ., 262, 118655, https://doi.org/10.1016/j.atmosenv.2021.118655, 2021.

Zhu, J., He, N., Wang, Q., Yuan, G., Wen, D., Yu, G., and Jia, Y.: The composition, spatial patterns, and influencing factors of atmospheric wet nitrogen deposition in Chinese terrestrial ecosystems, Sci. Total Environ., 511, 777-785, https://doi.org/10.1016/j.scitotenv.2014.12.038, 2015.